

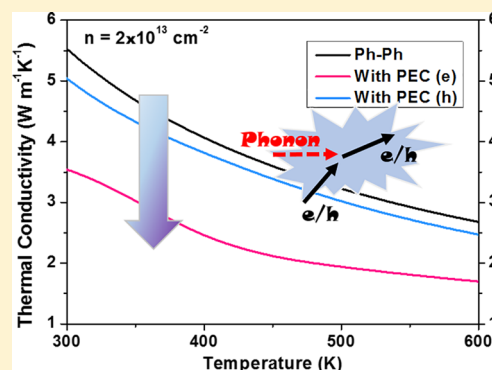
# Reducing Lattice Thermal Conductivity of the Thermoelectric SnSe Monolayer: Role of Phonon–Electron Coupling

Yajing Sun,<sup>1</sup> Zhigang Shuai,<sup>1</sup> and Dong Wang\*<sup>1</sup>

MOE Key Laboratory of Organic Opto Electronics and Molecular Engineering, Department of Chemistry, Tsinghua University, Beijing 100084, PR China

## Supporting Information

**ABSTRACT:** SnSe-based materials possess ultrahigh thermoelectric efficiency and show great potential in next-generation thermoelectric devices. The excellent thermoelectric performance of SnSe has been attributed to its ultralow lattice thermal conductivity. In addition to phonon–phonon interactions, grain boundary, and defect and impurity scatterings, phonon–electron coupling also plays a part in the lattice thermal transport of doped materials, yet it is often overlooked. In this work, we investigated the effect of phonon–electron coupling on the lattice thermal conductivity of the thermoelectric SnSe monolayer. We found that the lattice thermal conductivity decreased by as much as 30% when the carrier density exceeded  $10^{13} \text{ cm}^{-2}$  (equivalent to carrier concentration of  $\sim 10^{20} \text{ cm}^{-3}$ ), showing the significant suppression effect. Such level of carrier concentration is often required for thermoelectric conversion, so the contribution of phonon–electron coupling to the reduction for lattice thermal conductivity is as much as other scattering mechanisms and needs to be accounted for engineering phonon transport of thermoelectric materials.



## 1. INTRODUCTION

In crystalline materials, lattice vibrations will destroy the periodic potential in which the electrons move and seriously impede the electrical transport. According to the solid-state theory, interactions between electrons and phonons constitute the main scattering mechanism in charge transport.<sup>1,2</sup> However, effect of such interactions on phonon transport properties, such as the lattice thermal conductivity, is often overlooked. It was well believed that the electron–phonon interactions can be safely neglected when phonon transport properties are cared for because charge carrier concentrations in semiconductors or insulators are extremely low.<sup>3</sup> However, the performance of semiconductor-based electronic devices is often improved by increasing the carrier concentration.<sup>4–6</sup> Nowadays, the carrier concentration of electronic materials can be manipulated to the level as high as  $10^{21} \text{ cm}^{-3}$  in bulk and  $10^{14} \text{ cm}^{-2}$  in two-dimensional systems via various doping methods.<sup>7–11</sup> Meanwhile, experiments also show that thermal conductivities of some materials, such as thermoelectric clathrate and  $\text{La}_3\text{Te}_{4-x}\text{M}_x$  ( $M = \text{Sb}, \text{Bi}$ ), vary significantly with the doping level.<sup>12–14</sup> The thermal conductivity of doped materials usually decreases with the increasing carrier concentration, which has been attributed to the introduction of new phonon scattering pathways via phonon–electron coupling (PEC). Recently, comprehensive theoretical studies of the effect of PEC on the lattice thermal conductivity have been conducted for single-crystal silicon and bulk SiC and SiGe.<sup>3,15–17</sup> It was found that suppression on phonon transport due to the PEC effect can be significant. With the

increase of carrier concentration, the phonon–electron scattering is becoming a scattering mechanism as important as the phonon–phonon scattering in the phonon transport. At the carrier concentration as high as  $\sim 10^{20} \text{ cm}^{-3}$ , the lattice thermal conductivity was reduced by more than 40% in the abovementioned materials. In a word, to account for the PEC-induced scattering is essential when the accurate prediction of lattice thermal conductivity is needed, especially in doped single-crystalline thermoelectric materials. In polycrystalline materials, grain boundary and defect scatterings are also important. In this work, we will address the PEC effect in two-dimensional materials, which is rarely studied.

In addition to the traditional substitution strategy used in bulk materials, many effective and convenient approaches of doping can be applied to low-dimensional materials, which include surface charge transfer, intercalation, and field-effect modulation.<sup>11</sup> As far as we know, the only research targeting the PEC effect on the phonon transport of low-dimensional materials, deals with silicon nanostructure, in which both boundary and phonon–electron scattering mechanisms were studied.<sup>18</sup> However, the rates of scattering in the nanostructure were not explicitly calculated, instead, they were assumed the same values as in the bulk silicon. As we know, because of their unique electronic structure and phonon dispersions arising from the quantum confinement effect, low-dimensional

Received: March 12, 2019

Revised: April 17, 2019

Published: April 18, 2019

materials often exhibit charge and thermal transport features quite different from their bulk counterpart.<sup>19–22</sup> Therefore, evaluating the PEC effect on the lattice thermal conductivity of low-dimensional materials is essential for the accurate prediction of their thermal transport properties.

SnSe is emerging as a high-performance thermoelectric material due to its ultralow lattice thermal conductivity.<sup>23</sup> Though controversies on the intrinsic thermal conductivity of SnSe single crystals exist,<sup>24</sup> the SnSe-based material is becoming a promising candidate for thermoelectric conversion. SnSe possesses a layered structure, and fabrication of multilayer and monolayer nanosheets as well as their electrical transport and thermoelectric properties has been reported.<sup>25,26</sup> In this work, by performing first-principles computation of PEC in the thermoelectric SnSe monolayer, we found that the phonon scattering due to PEC cannot be neglected in two-dimensional systems, as it has been previously disclosed in bulk systems, especially at high carrier concentrations. The PEC-induced suppression of thermal conductivity increases with the carrier concentration. When the carrier density reaches  $10^{13} \text{ cm}^{-2}$  (equivalent to carrier concentration of  $\sim 10^{20} \text{ cm}^{-3}$ ), the lattice thermal conductivity can be reduced by as much as 30%. According to our calculation, the reduction of lattice thermal conductivity due to PEC is more dramatic in the SnSe monolayer than bulk. Our study points out that in the doping optimization of thermoelectric materials, the lattice thermal conductivity is no longer a constant and it decreases with increasing doping level due to the PEC effect, which is actually beneficial to achieve high thermoelectric efficiency.

## 2. METHOD

The structural optimization and electronic band structure calculation were performed based on the density functional theory implemented in Quantum Espresso package with the exchange–correlation functional of Perdew–Burke–Ernzerhof.<sup>27</sup> The density functional perturbation theory (DFPT) was then employed to calculate the phonon properties and the electron–phonon coupling matrix elements. The lattice thermal conductivity can be determined by solving the phonon Boltzmann transport equation via

$$\kappa = \sum_s^{3n} \int_q v_{q,s}^2 c_{q,s} \tau_{q,s} dq \quad (1)$$

where  $n$  is the number of atoms in the unit cell,  $v_{q,s}$ ,  $c_{q,s}$ , and  $\tau_{q,s}$  are, respectively, the phonon group velocity, heat capacity, and phonon lifetime of the  $s$ th phonon mode with wave vector  $q$ . In our calculation, the overall phonon lifetime is obtained by applying Matthiessen's rule to both phonon–phonon scattering mechanism arising from anharmonic lattice vibrations and PEC scattering mechanism<sup>1</sup>

$$\frac{1}{\tau_{q,s}} = \frac{1}{\tau_{q,s}^{\text{PP}}} + \frac{1}{\tau_{q,s}^{\text{PEC}}} \quad (2)$$

The phonon–phonon scattering was calculated by the ShengBTE package in the approximation of three-phonon scattering.<sup>28</sup> The second-order and third-order interatomic force constants were calculated using the  $5 \times 5$  supercell. From these, we could obtain the scattering matrix elements  $V_{ss's''}^{\pm}$ . According to Fermi's golden rule, phonon–phonon scattering rates  $\Gamma_{ss's''}^{\pm}$  can be written as

$$\Gamma_{ss's''}^{\pm} = -\frac{\hbar\pi}{4} \left\{ \frac{n' - n''}{n' + n'' + 1} \right\} \frac{\delta(\omega \pm \omega' - \omega'')}{\omega\omega'\omega''} |V_{ss's''}^{\pm}|^2 \quad (3)$$

In doped systems, the phonon lifetimes due to PEC scattering can be written as

$$\frac{1}{\tau_{q,s}^{\text{PEC}}} = -\frac{2\pi}{\hbar} \sum_{mn,k} |g_{mn,s}(k, q)|^2 \times (f_{nk} - f_{mk+q}) \times \delta(\varepsilon_{nk} - \varepsilon_{mk+q} - \hbar\omega_{qs}) \quad (4)$$

where  $g_{mn,s}(k, q) = \langle \psi_{mk+q} | \partial V | \psi_{nk} \rangle$  is the electron–phonon coupling matrix element. In order to simplify the calculation, the electron–phonon matrix elements on the dense grid were derived with the help of Wannier interpolation as implemented in the EPW code.<sup>29</sup> The electronic band energy, phonon energy, and electron–phonon matrix elements were first calculated on coarse  $k$ - and  $q$ -meshes of  $5 \times 5$ , respectively, and then interpolated to a fine grid of  $400 \times 400$ .

## 3. RESULTS AND DISCUSSION

**3.1. Geometry and Electronic Band Structure.** SnSe crystallizes in two phases, the  $Pnma$  phase below 750 K and the  $Cmcm$  phase above. In this work, we choose the low-temperature  $Pnma$  phase for our first-principles calculation. The monolayer of SnSe could be stripped easily from its bulk because of the weak interlayer van der Waals interactions.<sup>30</sup> The optimized structure of the SnSe monolayer is shown in Figure 1a. Each Sn atom is covalently bonded to three nearest

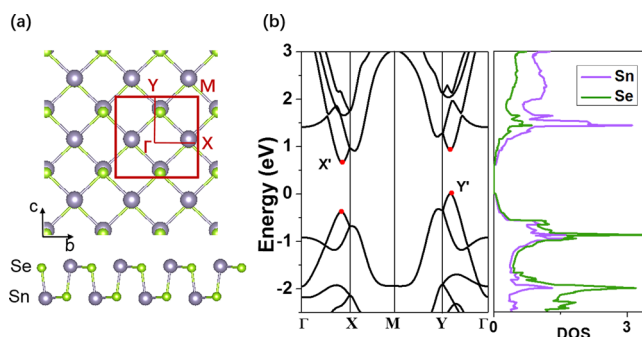


**Figure 1.** (a) Top and side views of the  $Pnma$  phase of the SnSe monolayer. (b) Electronic band structure and density of states of the SnSe monolayer.

Se atoms, forming a wrinkled structure. The orthogonal lattice is similar to that of puckered phosphorene and arsenene, with the optimized lattice parameters of 4.19 and 4.46 Å along the two orthogonal directions, respectively. Because the lattice parameters and atomic structures in the two directions are close to each other, the transport anisotropy of the SnSe monolayer is not as significant as it is in phosphorene and arsenene.

Figure 1b shows the electronic band structure and density of states. The SnSe monolayer is a semiconductor with an indirect band gap of 0.65 eV, which is larger than the bulk one of 0.48 eV because of the lack of interlayer van der Waals interactions. The band gap enlargement has been also observed in other materials with layered structures, such as in transition-metal chalcogenides.<sup>31</sup> By analyzing the density of states, we see that the valence band (VB) maximum is composed mainly of the Se element and the conduction band (CB) minimum is

composed of the Sn atom. The charge separation of VB and CB is caused by the electronegativity difference of Se and Sn atoms, with Se ( $p^4$ ) being the electron acceptor and Sn ( $p^2$ ) being the electron donor.

**3.2. Phonon–Phonon Scattering.** We calculated the phonon dispersion under the harmonic approximation and the three-phonon scattering rate using the third-order force constants of the SnSe monolayer. From the phonon dispersion plot (Figure 2), no obvious phonon band gap (acoustic–

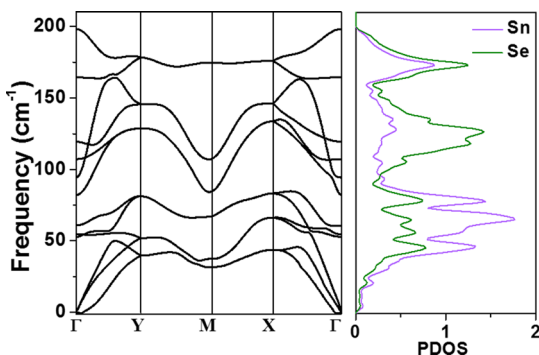


**Figure 2.** Phonon dispersion and phonon density of states of the SnSe monolayer.

optical gap) was observed, which may result in much stronger phonon–phonon scattering than other high thermal conductivity materials like cubic III–V compounds or puckered phosphorene. As shown in Figure 3, the three-phonon scattering rates range from  $10^{-3}$  to  $10$   $\text{ps}^{-1}$ , which are about 2 orders of magnitude larger than those in the III–V compound boron arsenide,<sup>32</sup> leading to the ultralow thermal conductivity in the SnSe monolayer.

In addition, from the distribution of phonon density of states, in the low-frequency region, Sn atoms contribute dominantly, while the high frequency phonons arise mainly from Se atoms. This is because of the larger mass of Sn atoms than Se. The phonon frequencies of SnSe are lower than other light-weight materials, so the phonon group velocities ( $v_{q,s} = \partial\omega_{q,s}/\partial q$ ) are also smaller. The phonon group velocities fall into the range of 1–2 km/s. This is another reason for the low thermal conductivity of SnSe. As mentioned before, the similar structure along the two perpendicular directions leads to the isotropic phonon dispersion and phonon group velocities. The predicted room-temperature thermal conductivity of the pristine SnSe monolayer is 5.58 and 5.01  $\text{W m}^{-1} \text{K}^{-1}$  along  $b$  and  $c$  directions, respectively. To obtain the thermal

conductivity of the monolayer, an effective thickness of 5.79 Å is taken, which is half of the out-of-plane lattice parameter in bulk SnSe. Figure 3c shows the accumulation of lattice thermal conductivity with the phonon mean free path. It can be seen that the phonon modes with the intrinsic mean free path of 0.5–10 nm contribute mostly to the lattice thermal conductivity of the SnSe monolayer.

**3.3. Phonon–Electron Coupling.** It is well-known that the electron–phonon coupling is essential to the charge transport. The charge carrier will be scattered from one state to another by absorbing or emitting a phonon, so its lifetime and mean free path are shortened. In the electron–phonon scattering process, the phonon lifetime and mean free path will also be further shortened if the charge carrier concentration is high. High-performance thermoelectric materials are often doped to increase the electrical conductivity, with the carrier concentration on the order of  $10^{20} \text{ cm}^{-3}$ . It has been pointed out that at such level of carrier concentration, the thermoelectric figure of merit could also be improved in both n- and p-doped situations by the reduction of lattice thermal conductivity.<sup>4,6</sup> In two-dimensions, the role of PEC in the phonon transport is not yet clarified. We calculated the PEC scattering rates in both n- and p-doped SnSe monolayers with the carrier density of up to  $10^{13} \text{ cm}^{-2}$ , and the result is shown in Figure 4. First, we find that at the carrier density of  $10^{13} \text{ cm}^{-2}$ , the rate of phonon–electron scattering is almost on the same order of magnitude as that of phonon–phonon scattering. Especially in the low-frequency region, the electron–phonon scattering rate even exceeds the phonon–phonon scattering rate, making PEC the leading phonon scattering pathway for the heat resistance. In both n- and p-doped cases, the phonon–electron scattering rates span a wide range between  $10^{-3}$  and  $1 \text{ ps}^{-1}$ . Second, we find that the PEC scattering rate in the case of electron doping is higher than that in the hole doping. To figure out the reason, we recall the band structure of the SnSe monolayer. As can be seen from Figure 1, there exist two energy valleys in the CB and two energy peaks in the VB along the high symmetry directions, and they are located near the X-point ( $X'$ ) and the Y-point ( $Y'$ ), respectively. We find that the energy difference between the two CB valleys is only 0.17 eV, which is much smaller than that between the two VB peaks, 0.37 eV. Because the phonon–electron scattering process needs to obey the conservation of both energy and momentum, the intervalley scattering of electrons (CB) is much easier than that of holes (VB). The above analysis can be further verified by the scattering rates decomposed as a function of both phonon frequency and

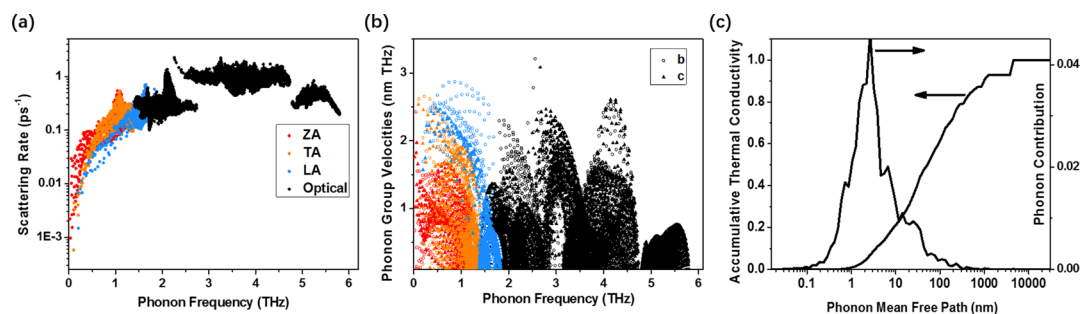


**Figure 3.** (a) Three-phonon scattering rates and (b) phonon group velocities of acoustic (ZA, TA, and LA) and optical modes as a function of the phonon frequency. (c) Accumulative lattice thermal conductivity at 300 K and respective phonon mode contribution decomposed with the phonon mean free path.

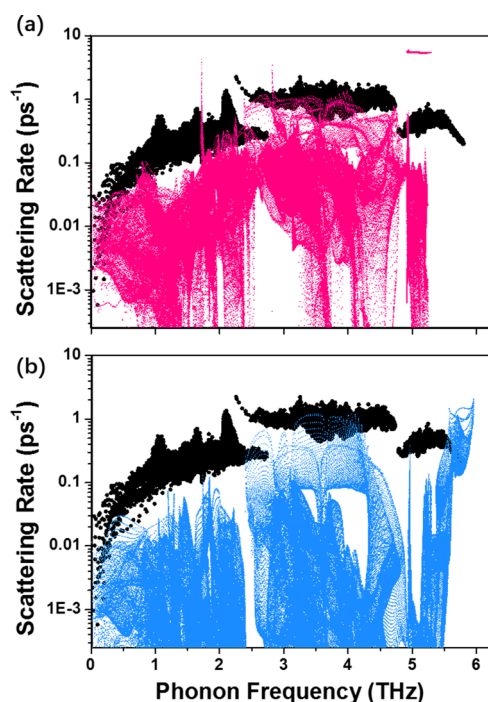


**Figure 4.** PEC scattering rates at (a) electron (pink dots) and (b) hole (blue dots) concentration of  $10^{13} \text{ cm}^{-2}$  as compared with three-phonon scattering rates (black dots).

phonon wave vector (Figure S1). It shows that in the regime of medium-to-large wave vectors, the scattering rate of electrons is high while that of holes is low. The overall scattering rate due to PEC in the n-doped monolayer of SnSe is obviously higher than that in p-doped one. Different from intravalley scatterings, intervalley scatterings are always mediated by phonon branches with medium-to-large wave vectors. In the large wave vector region, many intervalley scatter paths are forbidden in the p-doping situation, leading to extremely small scattering rates. Therefore, the main reason for the low PEC scattering rate in the p-doped SnSe is the larger energy difference between the two energy tops of VB, which suppresses the intervalley scattering.

The lattice thermal conductivity of the SnSe monolayer at 300 K, which varies with the carrier concentration, is shown in Figure 5a. At low carrier densities ( $<10^8 \text{ cm}^{-2}$ ), the scattering effect due to PEC in both n- and p-doped systems is not

obvious as compared to the phonon–phonon scattering. However, with the increase of carrier density, the effect gradually demonstrates. As the carrier density exceeds  $10^{12} \text{ cm}^{-2}$ , the PEC scattering starts to suppress the lattice thermal conductivity significantly. When the carrier density reaches  $10^{13} \text{ cm}^{-2}$ , the lattice thermal conductivity can be reduced by more than 30%. It shows that the PEC effect cannot be neglected for the accurate prediction of lattice thermal conductivity in two-dimensional materials at relatively high carrier densities, and to discern the critical carrier density above which PEC is not negligible, we introduce a parameter called the effective electron distance. We assume that charge carriers (electrons or holes) in the doped two-dimensional system are distributed evenly in the plane and the average distance between two adjacent carriers is defined as the effective electron distance. At low carrier densities, the effective distance is large, which means that the average distance between two neighboring electrons is large. If this effective distance is longer than the intrinsic phonon mean free paths that have the largest contribution to the total thermal conductivity (2–10 nm for the SnSe monolayer as shown above in Figure 3c), the phonon transport will not be significantly hindered by PEC. However, with the increase of carrier density, the effective distance between charge carriers decreases. In this case, one can imagine that the phonon will encounter and collide with the electron before it is scattered by other phonons. Therefore, if the effective electron distance is less than 10 nm, amounting to the carrier density of more than  $10^{12} \text{ cm}^{-2}$ , we have to account for the effect of PEC on the thermal transport. At this carrier density, the phonon scattering contributed by PEC is as much as 10%. The similar rule of thumb can also be applied to the bulk SnSe single crystal (Supporting Information Figure S3). Compared to the bulk system, the phonon mean free path in the monolayer is even longer, which indicates that the thermal conductivity in the doped SnSe monolayer is more prone to PEC. In a previous study of PEC effect on the phonon transport in the silicon nanostructure, it was concluded that the lattice thermal conductivity reduction due to PEC is not significant even at the carrier concentration as high as  $10^{21} \text{ cm}^{-3}$ .<sup>3</sup> The reason could be that in the nanostructure, the boundary scattering is the dominating scattering mechanism. As we show in this study, the PEC scattering plays an important role in the thermal transport of two-dimensional materials when the

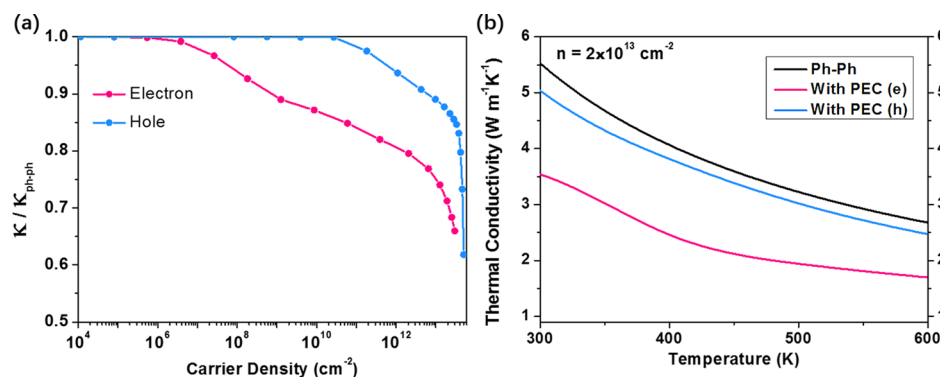


**Figure 5.** (a) Normalized lattice thermal conductivity as a function of the carrier density at 300 K.  $\kappa_{\text{ph-ph}}$  represents the lattice thermal conductivity arising from only phonon–phonon interaction. (b) Lattice thermal conductivity changing with the temperature at the hole and electron density both of  $2 \times 10^{13} \text{ cm}^{-2}$ .

carrier concentration reaches a level often seen in thermoelectric materials.

We have also explored the temperature dependence of lattice thermal conductivity with and without the inclusion of PEC scattering. From Figure 5b, we can see that the lattice thermal conductivity of single-layered SnSe is inversely proportional to the temperature when only phonon–phonon scattering is considered. After the electron–phonon scattering is taken into account, the lattice thermal conductivity decreases more rapidly and deviates from the inversely proportional dependence on the temperature.

#### 4. CONCLUSIONS

Based on the DFPT and Wannier interpolation method, we studied the effect of PEC on the lattice thermal conductivity of the thermoelectric SnSe monolayer. As in bulk materials, we found that PEC plays a significant role in the lattice thermal conduction of two-dimensional materials at high carrier concentrations. Specifically, when the carrier density reaches  $10^{13} \text{ cm}^{-2}$ , equivalent to the carrier concentration of  $\sim 10^{20} \text{ cm}^{-3}$ , the lattice thermal conductivity will be reduced by more than 30%, which could further enhance the thermoelectric efficiency of materials. The effective charge distance, which can be easily derived from the carrier concentration, was proposed to gauge the importance of PEC in the lattice thermal transport. When this effective charge distance is reduced to a value comparable to the intrinsic phonon mean free paths, which contribute mostly to the heat conduction of undoped materials, the PEC effect on the lattice thermal conductivity cannot be ignored. Because of the quantum confinement effect, the lattice thermal transport is more sensitive to PEC in low-dimensional SnSe than its bulk.

#### ■ ASSOCIATED CONTENT

##### Supporting Information

The Supporting Information is available free of charge on the ACS Publications website at DOI: 10.1021/acs.jpcc.9b02344.

PEC scattering rates as a function of phonon frequency and wave vector in monolayer SnSe and PEC effect in the SnSe single crystal (PDF)

#### ■ AUTHOR INFORMATION

##### Corresponding Author

\*E-mail: dong913@tsinghua.edu.cn.

##### ORCID

Yajing Sun: 0000-0003-2807-9382

Zhigang Shuai: 0000-0003-3867-2331

Dong Wang: 0000-0002-0594-0515

##### Notes

The authors declare no competing financial interest.

#### ■ ACKNOWLEDGMENTS

This work is supported by the National Natural Science Foundation of China (grant no. 21673123) and the Ministry of Science and Technology of China (grant nos. 2015CB655002 and 2017YFA020451). Computational resources are provided by the Tsinghua Supercomputing Center.

#### ■ REFERENCES

(1) Ziman, J. M. *Electrons and Phonons: The Theory of Transport Phenomena in Solids*; Clarendon Press: Oxford, 1960.

(2) Xi, J.; Wang, D.; Yi, Y.; Shuai, Z. Electron-Phonon Couplings and Carrier Mobility in Graphynes Sheet Calculated Using the Wannier-Interpolation Approach. *J. Chem. Phys.* **2014**, *141*, 034704.

(3) Liao, B.; Qiu, B.; Zhou, J.; Huberman, S.; Esfarjani, K.; Chen, G. Significant Reduction of Lattice Thermal Conductivity by the Electron-Phonon Interaction in Silicon with High Carrier Concentrations: A First-Principles Study. *Phys. Rev. Lett.* **2015**, *114*, 115901.

(4) Duong, A. T.; Nguyen, V. Q.; Duvjir, G.; Duong, V. T.; Kwon, S.; Song, J. Y.; Lee, J. K.; Lee, J. E.; Park, S.; Min, T.; et al. Achieving Zt=2.2 with Bi-Doped N-Type Snse Single Crystals. *Nat. Commun.* **2016**, *7*, 13713.

(5) Zhao, L.-D.; Tan, G.; Hao, S.; He, J.; Pei, Y.; Chi, H.; Wang, H.; Gong, S.; Xu, H.; Dravid, V. P.; et al. Ultrahigh Power Factor and Thermoelectric Performance in Hole-Doped Single-Crystal Snse. *Science* **2016**, *351*, 141–144.

(6) Chen, C.-L.; Wang, H.; Chen, Y.-Y.; Day, T.; Snyder, G. J. Thermoelectric Properties of P-Type Polycrystalline Snse Doped with Ag. *J. Mater. Chem. A* **2014**, *2*, 11171–11176.

(7) Korkosz, R. J.; Chasapis, T. C.; Lo, S.-h.; Doak, J. W.; Kim, Y. J.; Wu, C.-I.; Hatzikraniotis, E.; Hogan, T. P.; Seidman, D. N.; Wolverton, C.; et al. High Zt in P-Type (Pbte)1-2x(Pbse)x(Pbs)x Thermoelectric Materials. *J. Am. Chem. Soc.* **2014**, *136*, 3225–3237.

(8) Zhang, Q.; Chere, E. K.; McEnaney, K.; Yao, M.; Cao, F.; Ni, Y.; Chen, S.; Opeil, C.; Chen, G.; Ren, Z. Enhancement of Thermoelectric Performance of N-Type Pbse by Cr Doping with Optimized Carrier Concentration. *Adv. Energy Mater.* **2015**, *5*, 1401977.

(9) Hippalgaonkar, K.; Wang, Y.; Ye, Y.; Qiu, D.; Zhu, H.; Wang, Y.; Moore, J.; Louie, S. G.; Zhang, X. High Thermoelectric Power Factor in Two-Dimensional Crystals of mos2. *Phys. Rev. B* **2017**, *95*, 115407.

(10) Liu, C.; Xiong, Y.; Huang, Y.; Tan, X.; Li, L.; Xu, D.; Lin, Y.-H.; Nan, C.-W. Fevbs-Based Amorphous Films with Ultra-Low Thermal Conductivity and High Zt: A Potential Material for Thermoelectric Generators. *J. Mater. Chem. A* **2018**, *6*, 11435–11445.

(11) Luo, P.; Zhuge, F.; Zhang, Q.; Chen, Y.; Lv, L.; Huang, Y.; Li, H.; Zhai, T. Doping Engineering and Functionalization of Two-Dimensional Metal Chalcogenides. *Nanoscale Horiz.* **2019**, *4*, 26–51.

(12) Bentien, A.; Christensen, M.; Bryan, J. D.; Sanchez, A.; Paschen, S.; Steglich, F.; Stucky, G. D.; Iversen, B. B. Thermal Conductivity of Thermoelectric Clathrates. *Phys. Rev. B: Condens. Matter Mater. Phys.* **2004**, *69*, 045107.

(13) Bentien, A.; Johnsen, S.; Iversen, B. B. Strong Phonon Charge Carrier Coupling in Thermoelectric Clathrates. *Phys. Rev. B: Condens. Matter Mater. Phys.* **2006**, *73*, 094301.

(14) May, A. F.; Flage-Larsen, E.; Snyder, G. J. Electron and Phonon Scattering in the High-Temperature Thermoelectric  $\text{cl}_3\text{te}_4\text{-Zmz}$  (M=Sb,Bi). *Phys. Rev. B: Condens. Matter Mater. Phys.* **2010**, *81*, 125205.

(15) Wang, T.; Gui, Z.; Janotti, A.; Ni, C.; Karandikar, P. Strong Effect of Electron-Phonon Interaction on the Lattice Thermal Conductivity in 3c-Sic. *Phys. Rev. Mater.* **2017**, *1*, 034601.

(16) Fan, D. D.; Liu, H. J.; Cheng, L.; Liang, J. H.; Jiang, P. H. A first-principles study of the effects of electron-phonon coupling on the thermoelectric properties: a case study of the SiGe compound. *J. Mater. Chem. A* **2018**, *6*, 12125–12131.

(17) Cheng, L.; Yan, Q.-B.; Hu, M. The Role of Phonon-Phonon and Electron-Phonon Scattering in Thermal Transport in Pdcoo2. *Phys. Chem. Chem. Phys.* **2017**, *19*, 21714–21721.

(18) Fu, B.; Tang, G.; Li, Y. Electron-Phonon Scattering Effect on the Lattice Thermal Conductivity of Silicon Nanostructures. *Phys. Chem. Chem. Phys.* **2017**, *19*, 28517–28526.

(19) Novoselov, K. S.; Geim, A. K.; Morozov, S. V.; Jiang, D.; Zhang, Y.; Dubonos, S. V.; Grigorieva, I. V.; Firsov, A. A. Electric Field Effect in Atomically Thin Carbon Films. *Science* **2004**, *306*, 666–669.

(20) Lindsay, L.; Broido, D. A.; Mingo, N. Flexural Phonons and Thermal Transport in Graphene. *Phys. Rev. B: Condens. Matter Mater. Phys.* **2010**, *82*, 115427.

(21) Venkatasubramanian, R.; Siivola, E.; Colpitts, T.; O'Quinn, B. Thin-film thermoelectric devices with high room-temperature figures of merit. *Nature* **2001**, *413*, 597–602.

(22) Qin, G.; Zhang, X.; Yue, S.-Y.; Qin, Z.; Wang, H.; Han, Y.; Hu, M. Resonant Bonding Driven Giant Phonon Anharmonicity and Low Thermal Conductivity of Phosphorene. *Phys. Rev. B* **2016**, *94*, 165445.

(23) Zhao, L.-D.; Lo, S.-H.; Zhang, Y.; Sun, H.; Tan, G.; Uher, C.; Wolverton, C.; Dravid, V. P.; Kanatzidis, M. G. Ultralow Thermal Conductivity and High Thermoelectric Figure of Merit in Snse Crystals. *Nature* **2014**, *508*, 373–377.

(24) Wei, P.-C.; Bhattacharya, S.; He, J.; Neeleshwar, S.; Podila, R.; Chen, Y. Y.; Rao, A. M. The Intrinsic Thermal Conductivity of Snse. *Nature* **2016**, *539*, E1–E2.

(25) Jiang, J.; Wong, C. P. Y.; Zou, J.; Li, S.; Wang, Q.; Chen, J.; Qi, D.; Wang, H.; Eda, G.; Chua, D. H. C.; et al. Two-Step Fabrication of Single-Layer Rectangular Snse Flakes. *2D Mater.* **2017**, *4*, 021026.

(26) Ju, H.; Kim, J. Chemically Exfoliated Snse Nanosheets and Their Snse/Poly(3,4-Ethylenedioxythiophene):Poly(styrenesulfonate) Composite Films for Polymer Based Thermoelectric Applications. *ACS Nano* **2016**, *10*, 5730–5739.

(27) Giannozzi, P.; Baroni, S.; Bonini, N.; Calandra, M.; Car, R.; Cavazzoni, C.; Ceresoli, D.; Chiarotti, G. L.; Cococcioni, M.; Dabo, I.; et al. Quantum Espresso: A Modular and Open-Source Software Project for Quantum Simulations of Materials. *J. Phys. Condens. Matter* **2009**, *21*, 395502.

(28) Li, W.; Carrete, J.; Katcho, N. A.; Mingo, N. Shengbte: A Solver of the Boltzmann Transport Equation for Phonons. *Comput. Phys. Commun.* **2014**, *185*, 1747–1758.

(29) Noffsinger, J.; Giustino, F.; Malone, B. D.; Park, C.-H.; Louie, S. G.; Cohen, M. L. EPW: A program for calculating the electron-phonon coupling using maximally localized Wannier functions. *Comput. Phys. Commun.* **2010**, *181*, 2140–2148.

(30) Chang, C.; Tan, G.; He, J.; Kanatzidis, M. G.; Zhao, L.-D. The Thermoelectric Properties of Snse Continue to Surprise: Extraordinary Electron and Phonon Transport. *Chem. Mater.* **2018**, *30*, 7355–7367.

(31) Radisavljevic, B.; Radenovic, A.; Brivio, J.; Giacometti, V.; Kis, A. Single-Layer Mos2 Transistors. *Nat. Nanotechnol.* **2011**, *6*, 147–150.

(32) Lindsay, L.; Broido, D. A.; Reinecke, T. L. First-Principles Determination of Ultrahigh Thermal Conductivity of Boron Arsenide: A Competitor for Diamond? *Phys. Rev. Lett.* **2013**, *111*, 025901.